

IRON LINE EMISSION AND TWO-COMPONENT SPECTRAL BEHAVIOR IN THE ASCA  
OBSERVATION OF THE SEYFERT 1 GALAXY NGC 7469MATTEO GUAINAZZI,<sup>1</sup> MASARU MATSUOKA,<sup>2</sup> LUIGI PIRO,<sup>3</sup> TATEHIRO MIHARA,<sup>2</sup>  
AND MAKOTO YAMAUCHI<sup>2,4</sup>

Received 1994 June 27; accepted 1994 September 9

## ABSTRACT

The results of spectral-temporal analysis of an ASCA observation of the nearby Seyfert 1 galaxy NGC 7469 are presented providing an unprecedented combination of broadband coverage and energy resolution. A narrow fluorescence line (Gaussian dispersion  $\sigma < 150$  eV) of neutral iron was detected with equivalent width (EW)  $\approx 120$  eV. The iron line appears incompatible with emission from a relativistic accretion disk. The presence of a soft excess below 0.8 keV is confirmed by the ASCA data. Moreover, this component cannot be accounted for by a warm absorber model. A good agreement with the data is obtained by modeling the soft excess either via a thermal component or by reflection by a mildly ionized medium. Correlated luminosity and spectral variability was clearly detected in the observation, the spectrum getting steeper when the luminosity increases. A detailed analysis suggests that this behavior may be due to differing degrees of variability of the soft and hard components.

*Subject headings:* galaxies: individual (NGC 7469) — galaxies: Seyfert — X-rays: galaxies

## 1. INTRODUCTION

The nearby ( $z = 0.017$ ) Seyfert 1 galaxy has been the subject of extensive X-ray observations, which show indications of a very complex spectral structure. Evidence of a excess soft emission was first observed by EXOSAT (Barr 1986) and subsequently confirmed by the *Einstein Observatory* (Turner et al. 1991). The soft excess was confirmed by two ROSAT pointed observations (November 1991, Turner, Weaver, & Mushotzky 1993; April 1992, Brandt et al. 1993) although these data did not permit an unambiguous spectral interpretation of this component. However, the 1991 November data suggested the presence of an emission line at  $\approx 0.63$  keV or alternatively an absorption edge at  $\approx 0.86$  keV, consistent with the results of a fit to the earlier *Einstein* data. At higher energy, *Ginga* observations revealed evidence for a 6.4 keV iron fluorescence line and spectral flattening above 10 keV (Piro, Yamauchi, & Matsuoka 1990). Spectral fits assuming a Compton reflection model (George & Fabian 1991; Matt, Perola, & Piro 1991) yielded a power-law photon index for the primary source continuum of  $\Gamma = 1.92 \pm 0.03$  (Piro et al. 1990) or  $\Gamma = 1.99^{+0.06}_{-0.05}$  (Nandra 1991), although the alternative of a partial covering model could not be ruled out for a continuum with  $\Gamma = 1.88 \pm 0.02$  (Piro et al. 1990).

## 2. OBSERVATION AND DATA REDUCTION

NGC 7469 was observed by ASCA in 1993 between November 24 04:23:08 (UT) and November 26 20:10:46 (UT) for a total usable exposure time of  $\sim 40$  ks. The ASCA satellite and

its instruments are described in detail in Tanaka, Inoue, & Holt (1994). The solid imaging spectrometers (SIS) were operating in Faint CCD-2 mode. The gas imaging spectrometers (GIS) were operating in PHA mode. The spectrum was derived from photons detected within a  $3'$  radius of the apparent centroid of the source.

The source count rate varied by a 40% factor within a time-scale of  $5 \times 10^4$  s or less. The light curve from the SIS0 detector in the full nominal energy band (0.35–10 keV) is shown in Figure 1. In the following we distinguish a high-luminosity phase (HL) for  $t < 7 \times 10^4$  s (mean count rate  $1.721 \pm 0.015$  counts  $s^{-1}$ ) and a low-luminosity phase (LL) for  $t > 7 \times 10^4$  s (mean count rate  $1.22 \pm 0.06$  counts  $s^{-1}$ ). A model fit to the spectrum assuming an absorbed power law + blackbody continuum (see § 3.2) yields 2–10 keV band fluxes of  $F_{HL} = 3.59 \times 10^{-11}$  ergs  $cm^{-2} s^{-1}$  and  $F_{LL} = 2.98 \times 10^{-11}$  ergs  $cm^{-2} s^{-1}$ . These correspond to a luminosity  $\sim 4 \times 10^{43}$  ergs  $s^{-1}$  for  $H_0 = 50$  km  $s^{-1}$  Mpc $^{-1}$ . The amplitude of variability is within the range of previous observations of NGC 7469 that showed variations of up to a factor of 2 in X-ray flux.

## 3. SPECTRAL ANALYSIS

Some spurious low-energy features have been reported for the SIS spectra. An absorption edge-like feature at  $E \approx 0.47$  keV is present in observations of some other active galactic nuclei (AGNs), including the “standard” calibration source 3C 273 (K. Mitsuda, private communication). We verified that a small bias change ( $\Delta E \approx 18$  eV) in the gain relation would flatten off this feature, leaving the spectrum above 0.6 keV unchanged. An oxygen line of near-Earth origin and contributing  $1.1 \times 10^{-5}$  photons  $cm^{-2} s^{-1}$  has also been discovered at  $E = 0.54$  keV (Gendreau et al. 1994). We consequently restrict the spectral analysis of the SIS data to the range 0.57–9 keV, unless otherwise specified. The analysis range for GIS is 0.8–10 keV.

A simple absorbed power-law fit of both detector spectra gives as a result a mean spectral index of  $\Gamma_{SIS} = 2.016 \pm 0.010$  and  $\Gamma_{GIS} = 1.975^{+0.015}_{-0.014}$  (weighted mean  $\Gamma = 2.003 \pm 0.008$ ). In

<sup>1</sup> Istituto di Fisica, Università di Palermo, via Archirafi 36, I-90123 Palermo, Italy. E-mail: guainazzi@ipamat.math.unipa.it; also Institute of Physics and Chemical Research, Saitama, Japan.

<sup>2</sup> The Institute of Physics and Chemical Research, 2-1 Hirosawa, Wako, Saitama 350-01, Japan. E-mail: matsuoka@rkn50.riken.go.jp.

<sup>3</sup> Istituto di Astrofisica Spaziale, C.N.R., via E. Fermi 21, T-00044 Frascati, Italy.

<sup>4</sup> Present address: Faculty of Engineering, Miyazaki University, Kihnadai-Nishi 1-1, Gakuen Miyazaki, 889-21 Japan.

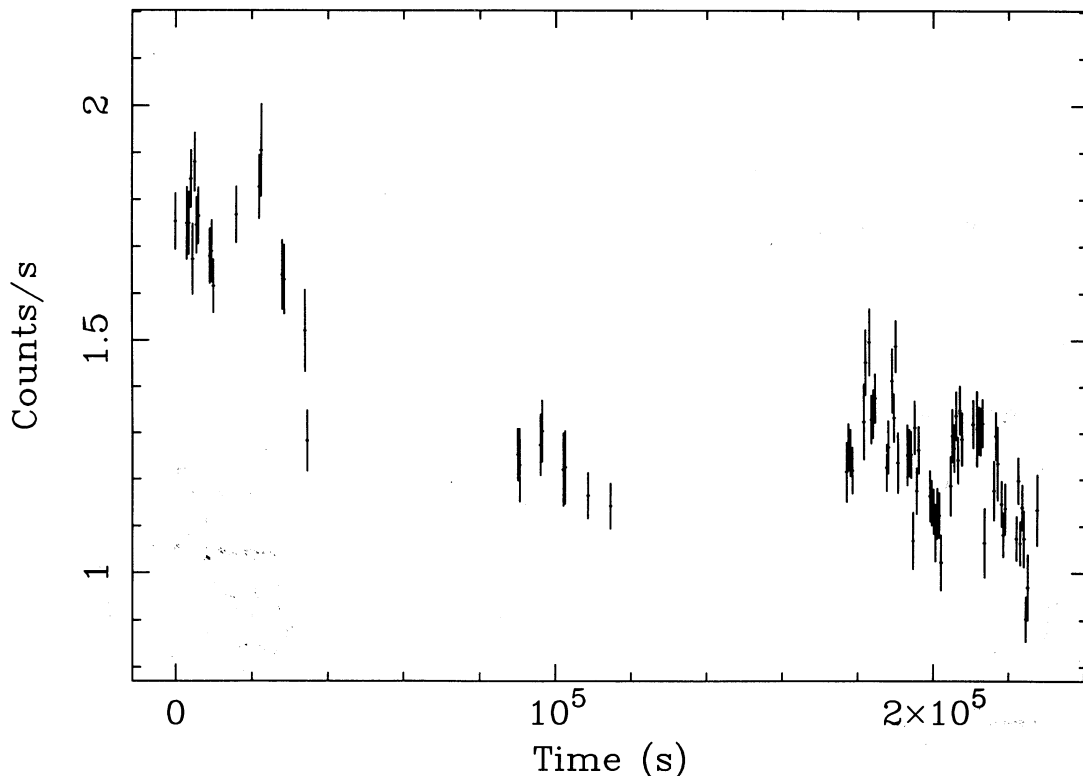


FIG. 1.—Light curve of ASCA NGC 7469 observation. Time is in seconds starting from 1993 November 24 04:59:29 (UT). Binning time is  $\Delta t = 500$  s. A flux variation of  $\sim 40\%$  is evident on a timescale of at most  $\sim 5 \times 10^4$  s.

the following, errors and upper limits are quoted at 90% confidence level for one interesting parameter (Lampton, Margon, & Boyer 1976). The hydrogen column density  $N_{\text{H}}$  has been held fixed to the Galactic value of  $5.3 \times 10^{20} \text{ cm}^{-2}$  (Dickey & Lockman 1990) in all the models employed in this Letter. The reduced  $\chi^2$  values for this fit are relatively high ( $\chi_r^2|_{\text{SIS}} = 1.36$ ,  $\chi_r^2|_{\text{GIS}} = 1.67$ ). As shown in Figure 2, the main contributions to high  $\chi^2$  are due to (1) excess emission below 0.8 keV; (2) line emission feature at  $E \simeq 6.3$  keV; and (3) large positive and negative residuals in the 1.8–2.3 keV energy interval, where the well-known Si K and Au M optics edges are present.

The result is in poor agreement with any previous result by EXOSAT, Ginga, and ROSAT. EXOSAT found a photon index  $\Gamma_{2-10 \text{ keV}} = 1.78 \pm 0.07$  (Turner & Pounds 1987), consistent with the result of Ginga in the same energy range,  $\Gamma_{2-10 \text{ keV}} = 1.83 \pm 0.01$  (Piro et al. 1990). In the softer 0.1–2.5 keV bandpass the two ROSAT observations yielded  $\Gamma_{0.1-2.5 \text{ keV}} = 2.50 \pm 0.08$  (1991 November) and  $\Gamma_{0.1-2.5 \text{ keV}} = 2.26 \pm 0.05$  (1992 April). These results suggest a spectral behavior more complicated than can be described by a single power law throughout the ASCA bandpass.

### 3.1. Iron Features

A fluorescent  $K\alpha$  line of neutral or weakly ionized iron is clearly detected in the spectrum of NGC 7469. Adding a Gaussian profile to the absorbed power-law model improves the fits to the spectra from the two detectors by  $\Delta\chi_{\text{SIS}}^2 = 26$  and  $\Delta\chi_{\text{GIS}}^2 = 23$ . The line centroid energy and equivalent width are  $E = 6.35 \pm 0.05$  keV and  $\text{EW} = 120 \pm 50$  eV for SIS and  $E = 6.51 \pm 0.15$  keV and  $\text{EW} = 110 \pm 40$  eV for GIS (here and thereafter the energies are quoted in the source frame). The SIS measurements take into account a 0.5% reduction in gain

below that assumed in the response matrices, which occurred for SIS0 in 1993 November (R. Fujimoto, private communication). The dispersion  $\sigma$  of the Gaussian profile is  $\leq 150$  eV.

These results have implications on the origin of the line. Since the line is narrow, it is unlikely that it is produced by a medium in relativistic motion around the central object. According to the computation of Matt et al. (1992a, b), the Fe  $K\alpha$  line produced by an accretion disk is expected to be narrower when the disk is seen face-on. Even in this case, however, the line width is expected to be greater than that observed in NGC 7469. Moreover, in this case, the line center is expected to be redshifted to  $E < 6.3$  keV.

The residuals of the SIS1 spectrum shows a further emission feature around  $E \simeq 6.8$  keV. Inclusion of a narrow line improves the fit by  $\Delta\chi^2 = 9$ , with resulting parameters  $E = 6.90^{+0.07}_{-0.04}$  keV and  $\text{EW} = 110 \pm 60$  eV. However, this feature in SIS0 spectrum is much weaker ( $\text{EW} = 60 \pm 50$  eV). Qualitatively it is tempting to interpret the lines at 6.4 and 6.9 keV as the double horn profile expected from an accretion disk, but a quantitative analysis shows poor agreement with theoretical predictions. Using the definitions given by equations (1)–(3) in Matt et al. (1992a) to describe the observed line profile, we have  $W_{\alpha} = 260 \pm 50$  eV,  $E_{\text{ca}} = 6.58 \pm 0.05$  keV, and  $\sigma_{\alpha} = 0.31 \pm 0.02$  keV. If  $\theta$  is the angle between the disk axis and the line of sight, the high centroid energy (in excess of the energy expected for neutral iron) is consistent with the broad maximum in line energy which occurs for  $70^\circ < \theta < 80^\circ$ . However, such a narrow width of the line complex can only be reconciled with small inclination angles; also, if we have underestimated the observed line width by as much as a factor of 2, the inclination angle must still be  $\theta < 45^\circ$ , with the X-ray

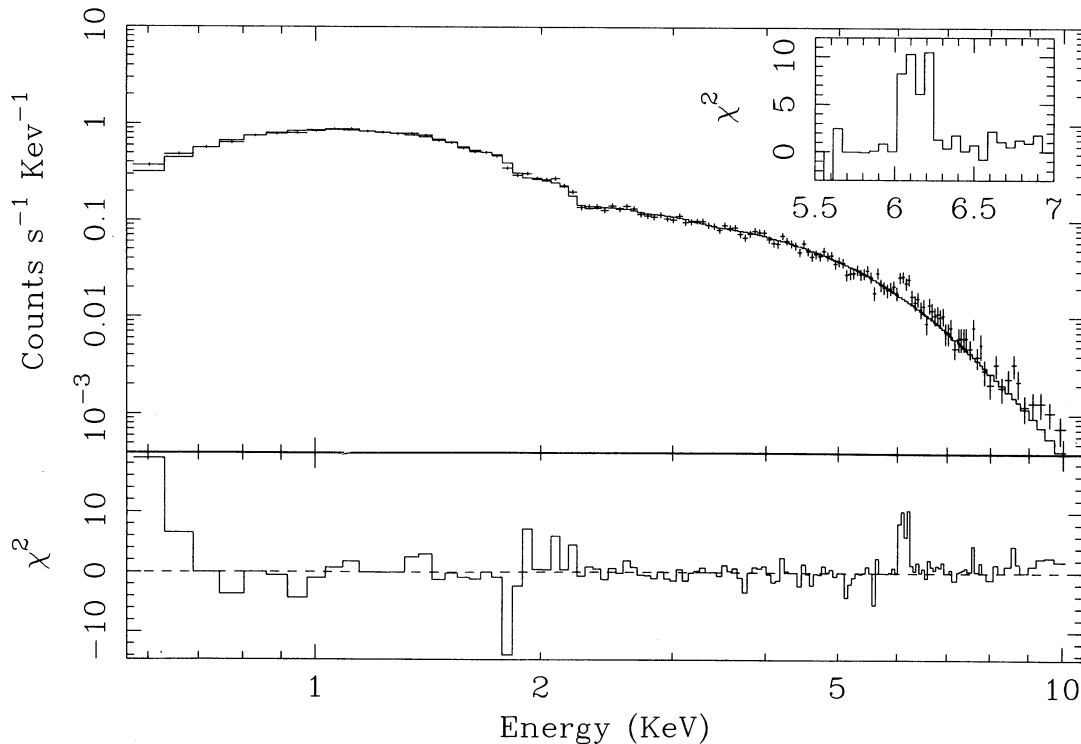


FIG. 2.—SIS0 spectrum fitted with an absorbed ( $N_{\text{H}} = N_{\text{Hgal}} = 5.3 \times 10^{20} \text{ cm}^{-2}$ ) power law (upper panel) and  $\chi^2$  contributions (lower panel). An excess component below 0.8 keV and line emission features at  $E \simeq 6.2$  keV (observer's frame) are clearly visible, together with residual jiggle around 2 keV, due to minor calibration errors.  $\chi_r^2 \simeq 1.4$ . The inset in the upper panel shows a blowup of the  $\chi^2$  contributions in the 6–7 keV interval.

source located  $\sim 50$  gravitational radii above the disk. Moreover, for any flat disk geometry the predicted EW does not exceed 180 eV. The observed Fe K $\alpha$  line parameters are thus in poor agreement with the theoretical predictions for the X-ray-illuminated cold relativistic disks.

The line EW can be increased up to a maximum value of  $\sim 270$  eV if reprocessing in a partially ionized medium is taken into account (Życki & Czerny 1994), but still it requires very broad emission (Matt, Fabian, & Ross 1993a). Moreover, iron K-edge absorption from such an ionized medium is not detected in the current data, and upper limits to this feature imply column densities that are factors of a few or more lower than expected [e.g.,  $N_{\text{HFe}}(\text{Fe xx}) < 6 \times 10^{22} \text{ cm}^{-2}$ ; see Piro, Matsuoka, & Yamauchi 1991]. An alternative explanation for the K $\alpha$  iron emission has been recently proposed as reprocessing by a system of cold clouds surrounding the central X-ray source (Bond & Matsuoka 1993; Nandra & George 1994), which could be consistent with a wider range of observed EWs; specific predictions about the line profile require assumptions on the distribution of the clouds around the central source and no detailed model is presently available.

In conclusion, whatever the exact geometrical configuration of the reprocessing matter may be in NGC 7469, the narrow width of the line indicates that the bulk of the emitting material cannot lie too close ( $R >$  several tens of Schwarzschild radii) to the central putative black hole.

### 3.2. Continuum Spectral Features

In order to understand the nature of the soft excess we have first estimated the shape of the spectrum above 2.5 keV, which

should be dominated by the intrinsic primary continuum in the SIS band. A fit with a simple power law yields  $\Gamma_{\text{HE}} = 1.92 \pm 0.03$ . This value is in good agreement with that observed by *Ginga* after the inclusion of the reflected component (Piro et al. 1990; Nandra 1991). Inclusion of a reflected component in the fit does not change significantly the value of the spectral index, yielding only a loose upper limit on the level of the reflected component.

No significant absorption feature on a simple power-law fit with spectral index free and the column density subject to the only constraint  $N_{\text{H}} > N_{\text{Hgal}}$  has been found. Upper limits on the optical depths of O VII and O VIII absorption edges are 0.07 and 0.05, respectively. Furthermore, no emission line can be fitted to the spectrum below 1 keV. These results argue against an explanation of the soft excess in terms of a warm absorber.

Thermal continuum model for the soft X-ray excess emission provide a much better fit for the NGC 7459 spectra. Combining a blackbody or a bremsstrahlung emission to the simple power law with  $\Gamma = 1.92$  and the Gaussian Fe K $\alpha$  line models provides a good fit to the overall spectrum ( $\chi^2 = 1.2$ ) with a further  $\Delta\chi^2 = 115$ . The temperature of the thermal component ( $80^{+19}_{-14}$  eV for blackbody,  $150 \pm 100$  eV for bremsstrahlung) is compatible with the value observed by *ROSAT* (Brandt et al. 1993).

An alternative and tempting explanation for the soft excess is by reflection from partially ionized matter (Matt, Fabian, & Ross 1993b) and has been recently applied to some Seyfert galaxies (Czerny & Życky 1994; Piro et al. 1994). If the ionizing flux is intense enough to leave most oxygen in a He- or H-like stage and H, He, and C fully ionized, matter becomes highly reflective below  $E \sim 0.8$  keV, corresponding to the absorption

edges of the prevailing ion species (O VII and O VIII) and absorbing above it. The NGC 7469 spectrum has been fitted with a rough approximation of the albedo, produced by a reflecting ionized slab in such physical conditions, of the form  $e^{-\sigma(E)N_{\text{H,ref}}}[C_1 + C_2 \Lambda(E, E_{\text{O VII}}) + C_3 \Lambda(E, E_{\text{O VIII}})]E^{\Gamma_{\text{HE}}} +$  narrow iron line, where  $\Lambda(E, E_{\text{edge}})$  assumes the values 1 for  $E < E_{\text{edge}}$  and 0 for  $E \geq E_{\text{edge}}$  and  $C_i$  are normalization constants. An acceptable fit is obtained ( $\chi^2 = 1.3$ ) with  $\Delta\chi^2 = 98$  compared to the simple power law + line. The relative normalization of the reflected component are  $C_2/C_1 = 0.13^{+0.04}_{-0.05}$  and  $C_3/C_1 = 0.03 \pm 0.03$ . These results indicate that O VII should be in such a model the prevailing stage of oxygen; this corresponds to an ionization parameter  $\zeta = 4\pi F(r)/n_{\text{H}}$  of order 50–100. This finding confirms that a reprocessing mildly ionized medium cannot extend too near to the central object ( $R$  about 50–100 $R_{\text{S}}$ ; Życki & Czerny 1994); otherwise, the ionization parameter would be much greater than 100.

#### 4. TEMPORAL ANALYSIS

We have examined the *ASCA*-data for spectral behavior that is correlated with intensity variability. The analysis presented in this section refers to SIS data only. We adopt a notation in which  $r_n$  is the linear correlation coefficient for  $n$  points,  $\chi_{\text{ch}}^2/\nu$  is the  $\chi^2$  value for the hypothesis of constant behavior, and  $P \equiv P_r(\chi^2 > \chi_{\text{ch}}^2)$  is the random occurrence likelihood for  $\chi^2 > \chi_{\text{ch}}^2$ , where  $\nu$  is the number of degrees of freedom.

A correlation between the hardness ratio (HR, defined as the ratio between the flux in 0.5–2.5 and 2.5–9 keV bands) and the count rate is present over the whole range of timescales between  $10^2$  and  $10^4$  s. For a binning time of  $\Delta t = 500$  s the linear correlation coefficient  $r_{81} = -0.30 \pm 0.09$  ( $\chi_{\text{ch}}^2 = 111/80$ ,

$P \sim 0.01$ ). Moreover, a strong anticorrelation was found between (2.5–5 keV)/(0.57–1.25 keV) ratio and total bandpass intensity ( $r_{23} = -0.54 \pm 0.10$ ,  $\chi_{\text{ch}}^2 = 42/22$  and  $P < 0.01$ ) intensity while little evidence of variability was present for the (5–9 keV)/(2.5–5 keV) ratio ( $r_{23} = -0.2 \pm 0.3$ ,  $\chi_{\text{ch}}^2 = 14/22$ ).

A more detailed analysis was performed by dividing the whole observation into eight parts, with each segment described by a usable exposure time  $\sim 5 \times 10^3$  s and number of counts greater than 4500. A plot representing the spectral photon index of a simple absorbed power-law model in the (0.57–0.8 keV) and (2.5–10 keV) energy bandpasses as a function of the total count rate is shown in Figure 3. The correlation between the former and intensity is highly significant, with  $r_7 = 0.94 \pm 0.18$  (random occurrence likelihood  $< 0.2\%$ ), while no correlation is evident between the latter and intensity ( $r_7 = 0.2 \pm 0.5$ ). The soft excess is clearly variable, being strong in the HL phase and only statistically marginal during the LL phase. The high-energy photon index instead remains fairly constant around the mean value  $\Gamma_{\text{HE}} = 1.93 \pm 0.03$ .

The results described above for NGC 7469 can be easily understood in terms of two-component behavior of the continuum emission such that the soft and hard components vary either with a different amplitude or on different timescales.

#### 5. DISCUSSION AND CONCLUSIONS

The unprecedented combination of broadband coverage and high spectral resolution provided by *ASCA* is shedding new light on the temporal and spectral properties of X-ray emission from AGNs. The results presented here provide support for an interpretation of the soft excess emission below  $E \sim 0.8$  keV as a thermal continuum component, rather than the result of a

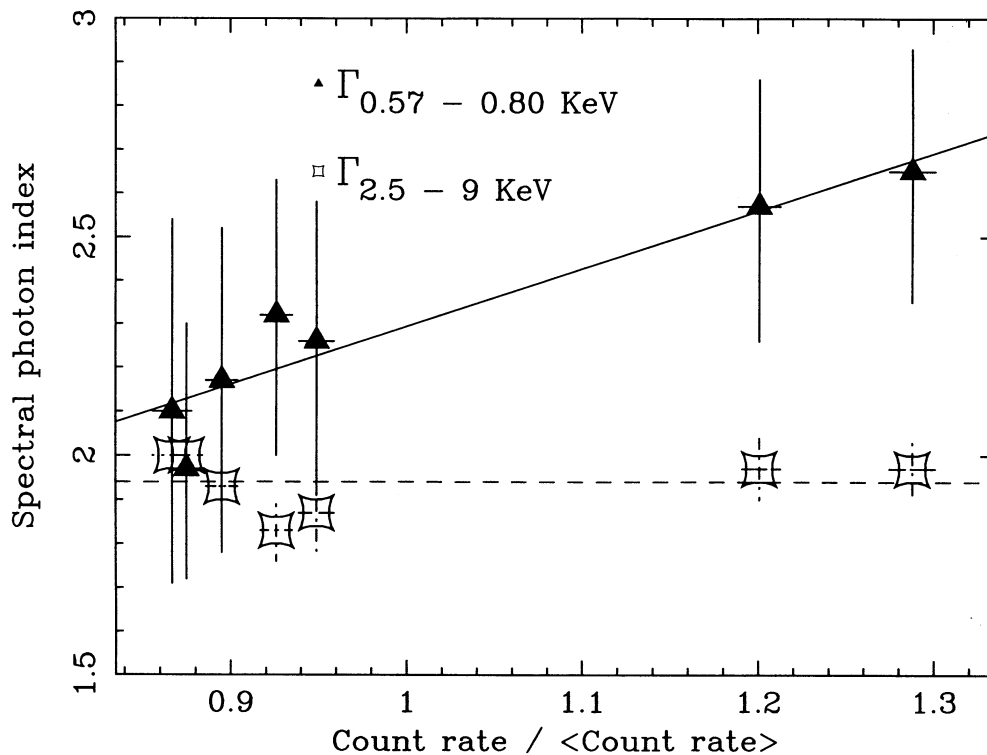


FIG. 3.—Spectral photon index in the (0.57–0.80 keV) (triangles) and (2.5–9 keV) (diamonds) ranges vs. count rate. The linear correlation coefficient are  $r_7 = 0.94 \pm 0.18$  [ $P(r > r_7) < 0.2\%$ ] and  $r_7 = 0.2 \pm 0.5$ , respectively. The continuous line is the linear fit to the (0.57–0.8 keV) indexes; the dashed line the constant best fit to the (2.5–9 keV) indexes.

warm absorber. This conclusion is further supported by the lack of detection of Fe absorption edges in the spectrum. An appealing alternative is provided via reflection by a partially ionized medium with an average ionization parameter 50–100.

The present observation confirms that the soft X-ray emission in the band 0.6–2.5 keV is variable with different amplitude or on a different timescale than the 2.5–10 keV band emission.

The iron  $K\alpha$  emission line presents a very narrow structure and no significant redshift. These characteristics are difficult to reconcile with predictions for the line profile emission originated by reflection from a relativistic accretion disk. The line-emitting region should consequently be located at distances

greater than several tens of Schwarzschild radii from the central source.

The authors would like to thank all members of the *ASCA* team and the launching staff at ISAS for successful *ASCA* data taking. Particular thanks to Maxim Markevitch for many enlightening discussions about the emission-line calibration problems in SIS detectors. The authors are deeply grateful to an anonymous referee for the careful revision of the *Letter*. M. G. acknowledges partial support from Ministero dell'Università e della Ricerca Scientifica e Tecnologica (MURST). L. P. acknowledges partial support from ASI.

## REFERENCES

- Barr, P. 1986, *MNRAS*, 223, 29P  
 Bond, I. A., & Matsuoka, M. 1993, *MNRAS*, 265, 619  
 Brandt, W. N., Fabian, A. C., Nandra, K., & Tsuruta, S. 1993, *MNRAS*, 265, 996  
 Czerny, B., & Życki, P. T. 1994, *ApJ*, 431, L5  
 Dickey, J. M., & Lockman, F. J. 1990, *ARA&A*, 28, 215  
 Gendreau, C. K., et al. 1994, in *New Horizon of X-Ray Astronomy: First Results from ASCA*, ed. F. Makino (Tokyo: Universal Academy), 365  
 George, I. M., & Fabian, A. C. 1991, *MNRAS*, 249, 352  
 Lampton, M., Margon, B., & Bowyer, S. 1976, *ApJ*, 208, 177  
 Matt, G., Fabian, A. C., & Ross, R. R. 1993a, *MNRAS*, 262, 179  
 ———. 1993b, *MNRAS*, 264, 839  
 Matt, G., Perola, G. C., & Piro, L. 1991, *A&A*, 247, 25  
 Matt, G., Perola, G. C., Piro, L., & Stella, L. 1992a, *A&A*, 257, 63  
 Matt, G., Perola, G. C., Piro, L., & Stella, L. 1992b, *A&A*, 263, 453  
 Nandra, K. 1991, Ph.D. thesis, Leicester Univ.  
 Nandra, K., & George, I. M. 1994, *MNRAS*, 267, 974  
 Piro, L., Balunconska-Church, M., Fink, H., Fiore, F., Matsuoka, M., Perola, G. C., & Soffitta, P. 1994, in preparation  
 Piro, L., Matsuoka, M., & Yamauchi, M. 1991, in *Physics of Active Galactic Nuclei*, ed. W. J. Duschl & S. J. Wagner (Heidelberg: Springer-Verlag), 45  
 Piro, L., Yamauchi, M., & Matsuoka, M. 1990, *ApJ*, 360, L35  
 Tanaka, Y., Inoue, H., & Holt, S. S. 1994, *PASJ*, 46, L37  
 Turner, T. J., & Pounds, K. 1989, *MNRAS*, 240, 833  
 Turner, T. J., Weaver, K. A., & Mushotzky, R. F. 1993, *ApJ*, 412, 72  
 Turner, T. J., Weaver, K. A., Mushotzky, R. F., Holt, S. S., & Madejski, G. M. 1991, *ApJ*, 381, 85  
 Życki, P. T., & Czerny, B. 1994, *MNRAS*, 266, 653